Journal of The Electrochemical Society, **151** (11) G746-G750 (2004)
0013-4651/2004/151(11)/G746/5/$7.00 © The Electrochemical Society, Inc.

Failure Mechanism of Amorphous and Crystalline Ta-N Films in the Cu/Ta-N/Ta/SiO_2 Structure

Ching-Chun Chang, J. S. Chen,[a,*,z] and Wu-Shiung Hsu[b]

[a]*Department of Materials Science and Engineering, National Cheng Kung University, Tainan, Taiwan*
[b]*Nuclear Science Technology Development Center, National Tsing Hua University, Hsinchu, Taiwan*

The diffusion barrier properties of as-deposited amorphous TaN_x ($x \approx 0.5$) and crystalline TaN between Cu and SiO_2 have been investigated in Cu/Ta-N/Ta/SiO_2 structures. The thermal reactions of Cu/TaN_x/Ta/SiO_2 and Cu/TaN/Ta/SiO_2 after annealing in vacuum at 500 to 900°C were investigated by using sheet resistance measurements, glancing incident angle X-ray diffraction, scanning electron microscopy, energy-dispersive X-ray spectrometry, and Rutherford backscattering spectrometry. No significant reaction and change of sheet resistance were detected for both systems after annealing up to 800°C. As compared to TaN, TaN_x exhibited better electrical properties and capability for preventing Cu diffusing through it. However, the sheet resistance of both systems increased abruptly after annealing at 900°C, especially the TaN_x system. The severe increase in sheet resistance corresponds to the deterioration of Cu surfaces. Broken holes were seen in the TaN_x layer, which were the initial sites for the structural failure. The cause of failure in Cu/Ta-N/Ta/SiO_2 stacks is discussed on the basis of the characteristics of Ta-N films upon heat-treatment.
© 2004 The Electrochemical Society. [DOI: 10.1149/1.1803836] All rights reserved.

Manuscript received June 11, 2003. Available electronically October 7, 2004.

With demands for an increase in the packing density and improvement in device performance, the linewidths of integrated circuits have reduced continuously to deep submicrometer dimensions. In ultralarge-scale integrated (ULSI) circuits, resistance-capacitance (RC) time delay and electromigration become the important issues. Consequently, aluminum-based metallurgy is no larger adequate for deep submicrometer metallization. In order to solve these problems, copper has been adopted as the interconnection metal because of its lower resistivity (1.67 μΩ cm) as compared with aluminum (2.7 μΩ cm). Meanwhile, the resistance to electromigration of copper is higher, also.[1-3] However, copper diffuses easily into Si and SiO_2 to form Cu-Si compounds at quite low temperatures.[4,5] This causes device performance to degrade seriously. To avoid copper diffusion, a barrier between copper and its underlying dielectric layer is essential. For copper metallization, diffusion barriers of refractory metals and their nitrides have been studied extensively owing to their superior thermal stability and high conductivity, including Ti-N,[6,7] Ta-N,[8-12] and W-N.[13-16] Among them, tantalum and its nitride draw lots of attention because they possess better thermal stability and chemical inertness than the other transition metal nitrides when coming into contact with copper.

However, tantalum nitride may be in the form of TaN or Ta_2N, and it can be crystalline or amorphous. Due to the different deposition conditions, the properties of tantalum nitride barriers can vary widely.[11,17-19] In the literature, most studies related with barrier performance concern only one tantalum nitride film of one specific composition and structure. In the present study, we deposited tantalum nitride film by reactive sputtering. Amorphous tantalum nitride films (TaN_x, $x \approx 0.5$) and polycrystalline tantalum nitride films (TaN) were obtained by changing the sputtering ambient. In addition, most of the literature reports concern the interactions of Cu films deposited on Ta-N/⟨Si⟩ substrates. However, the interactions of Cu with the Ta-N/SiO_2/⟨Si⟩ structure should be more relevant to the current Cu interconnect system. Therefore, we compared the reactions in the two types of Cu/Ta-N(TaN_x or TaN)/Ta/SiO_2/⟨Si⟩ (⟨Si⟩ represents the single-crystal Si substrate) stacks after annealing at 500 to 900°C.

Sheet resistance, phases, elemental depth profiles, and surface morphology of the samples were examined. All these analyses could give us a guideline for the selection of the tantalum nitride as the diffusion barrier in the ULSI devices.

* Electrochemical Society Active Member.
z E-mail: jenschen@mail.ncku.edu.tw

Experimental

The substrates used in the present study were n-type (100) Si wafers with resistivity of 1-10 Ω cm. The substrates were immersed in an organic bath and chemically etched with dilute HF solution ($HF:H_2O = 1:10$). Thermal SiO_2 film, 280 nm in thickness, was grown by oxidizing Si wafers in dry oxygen at 1050°C. Ta-N films, 50 nm in thickness, were deposited by radio frequency (rf) sputtering from a Ta metal (99.95% purity) target in different nitrogen-argon mixed ambients and applied with a negative substrate bias of −100 V. The films prepared with 1 and 5% of nitrogen flow ratio $[N_2/(N_2 + Ar)]$ are amorphous TaN_x ($x \approx 0.5$) and polycrystalline TaN, respectively. More detailed information about the Ta-N films can be found in our previous work.[20] Before Ta-N deposition, a 10 nm thick Ta layer was deposited to improve the adhesion between Ta-N and SiO_2 layer. Cu films (180 nm) were then deposited on Ta-N films using dc sputtering with a Cu target (99.99% purity). The two groups of Cu/Ta-N/Ta/SiO_2/⟨Si⟩ samples were then annealed side by side in vacuum (2.5×10^{-5} Torr) at temperatures ranging from 500 to 900°C for 30 min to investigate thermal interactions. Sheet resistances of all samples, before and after annealing, were measured with a four-point probe. The crystalline structures of Cu/Ta-N/Ta/SiO_2/⟨Si⟩ were characterized by using glancing incident angle X-ray diffraction (GIAXRD, Rigaku D/MAX2500) at an incident angle of 2° with Cu Kα radiation. Surface morphology of the films was examined by scanning electron microscopy (SEM, Philips XL-40FEG). The variations of surface compositions were estimated by energy dispersive X-ray spectrometry (EDS, Philips EDAXDX-4). Depth profile analysis was performed with Rutherford backscattering spectrometry (RBS). For RBS measurement, the $^4He^+$ ions were accelerated to 2 MeV and the backscattered ions were detected at a scattering angle of 160°.

Results and Discussion

The sheet resistances of all the samples, before and after annealing, were characterized by a four-point probe and presented in Fig. 1. The sheet resistance values of Cu/TaN_x/Ta/SiO_2/⟨Si⟩ samples were lower than those of Cu/TaN/Ta/SiO_2/⟨Si⟩ samples upon annealing to 900°C, which might be due to the lower resistivity of TaN_x (~200 μΩ cm) than that of TaN (~340 μΩ cm), and fewer defects in the films before annealing at high temperature. In general, the measured sheet resistance was dominated by the copper film since the resistivity of copper is much lower than that of Ta-N film. Therefore, the variations of the measured sheet resistance may represent the changes in the structure or composition of Cu film, or the intermixing degree of copper film with the underlayer.

DOCKET ALARM
Find authenticated court documents without watermarks at docketalarm.com.

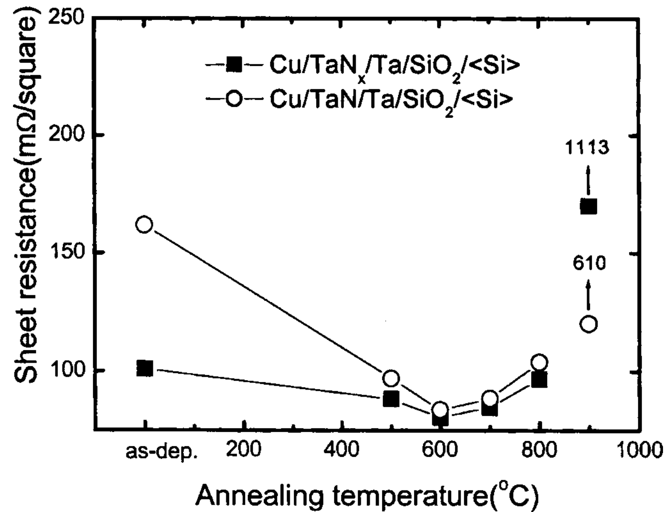

Figure 1. Dependence of sheet resistance of Cu/Ta-N/Ta/SiO_2/⟨Si⟩ samples on the annealing temperatures.

The sheet resistance values of both systems decreased with increasing annealing temperatures until 600°C. It is mainly attributed to copper grain growth and the self-healing effect of defects in the Cu film. After annealing at 700°C or above, however, the sheet resistance values rise slightly as the annealing temperature increases. After annealing at 900°C, the sheet resistance of the Cu/TaN_x/Ta/SiO_2/⟨Si⟩ sample increased dramatically to 1113 mΩ/□ and that of the Cu/TaN/Ta/SiO_2/⟨Si⟩ sample increased to 610 mΩ/□. To further understand the mechanisms that made the differences in these two systems, several material characterizations were carried out as follows.

Figure 2 presents the GIAXRD patterns of Cu/TaN_x/Ta/SiO_2/⟨Si⟩ and Cu/TaN/Ta/SiO_2/⟨Si⟩ samples before and after annealing at 500-900°C. Copper diffraction peaks and a broad peak at $2\theta \approx 37°$ are seen in the as-deposited Cu/TaN_x/Ta/SiO_2/⟨Si⟩ sample (Fig. 2a), indicating that the TaN_x layer is amorphous. The crystallization temperature of amorphous TaN_x has been determined by annealing the film at temperatures from 300 to 900°C in 100°C intervals. This indicates that the TaN_x layer began to crystallize into a Ta_2N phase after annealing at 500°C. In Fig. 2b, only the diffraction peaks of TaN and Cu were observed in the as-deposited and 500°C-annealed samples. However, we can find the Ta_2N(100) (at $2\theta \approx 34°$) and Ta_2N(101) (at $2\theta \approx 39°$) diffraction peaks in the pattern of the 600°C annealed sample. According to the composition obtained by RBS analysis, the TaN film on a graphite substrate showed the composition of $Ta_{48}N_{52}$. Therefore, the existing Ta_2N phase after annealing at 600°C is attributed to the reaction of the thin Ta underlayer with the excess nitrogen atoms in the TaN film. After annealing at 900°C, the intensities of Cu diffraction peaks decreased in both the Cu/Ta-N/Ta/SiO_2/⟨Si⟩ systems, which might be attributed to the diffusion of copper into the underlayer and reaction with the silicon to form copper silicide.

SEM micrographs on the surfaces of both Cu/TaN_x/Ta/SiO_2/⟨Si⟩ and Cu/TaN/Ta/SiO_2/⟨Si⟩ samples after annealing at 700, 800, and 900°C are shown in Fig. 3 and 4. The surfaces of Cu/TaN_x and Cu/TaN systems after annealing at 700°C simply show the morphology of Cu grains (Fig. 3a and b). After annealing at 800°C, broken holes are evident on the copper surfaces which appeared in the Cu/TaN_x systems (Fig. 3c). However, there were only tiny voids observed in the Cu/TaN system (Fig. 3d). It is observed that Cu grains started to agglomerate after annealing at 700°C in this study. Moreover, holes and voids formed on the 800°C-annealed samples would increase the sheet resistance further. The rough surface morphology of Cu correlated well with the increases in the sheet resistance (Fig. 1) in both Cu/TaN_x and Cu/TaN systems.

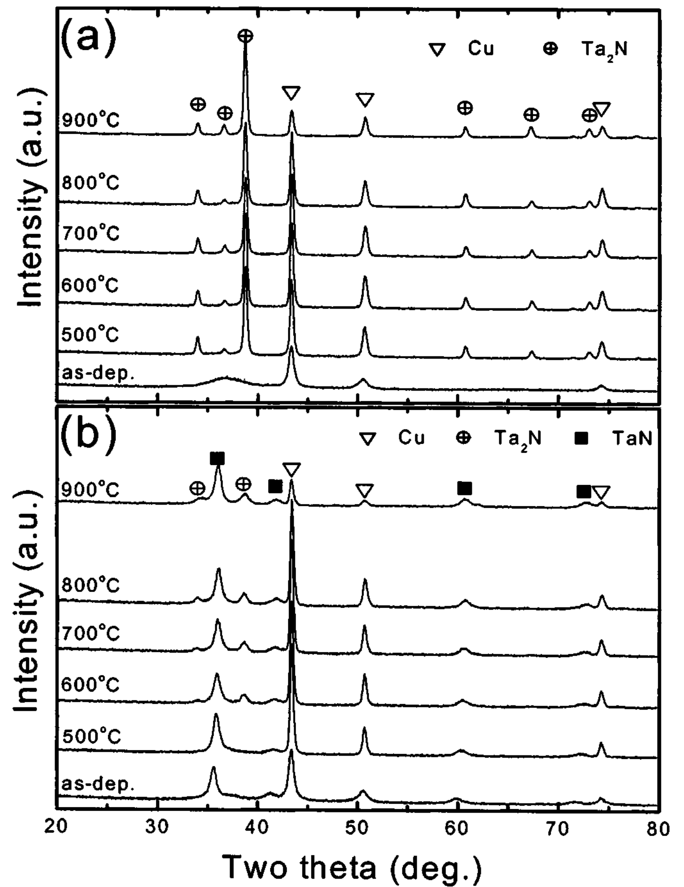

Figure 2. GIAXRD patterns of (a) Cu/TaN_x/Ta/SiO_2/⟨Si⟩ and (b) Cu/TaN/Ta/SiO_2/⟨Si⟩ samples as deposited and after annealing at 500, 600, 700, 800, and 900°C.

After annealing at 900°C, gray dots could be seen with the naked eye on the surface of the Cu/TaN_x sample. The gray dots under SEM can be represented by the micrograph of Fig. 4a and the dark region at the center seems to be a broken area. On the other hand, the surface of the Cu/TaN system under SEM exhibited a circular region of different contrast but no broken area (Fig. 4b). Except for the gray spots, the surface morphology of the other areas on the Cu/TaN_x system was basically similar to the Cu/TaN system. SEM analysis indicates that more severe local reaction occurred in the Cu/TaN_x/Ta/SiO_2/⟨Si⟩ stack than the Cu/TaN/Ta/SiO_2/⟨Si⟩ stack after annealing at 900°C. Comparing the surface morphology of Cu/TaN_x and Cu/TaN systems, we can conclude that there must be local defects originally existing in both TaN_x and TaN films. Upon 900°C annealing, the local defects in the TaN_x film would change into apparent holes, but this phenomenon did not happen in the TaN film. The reasons for the diversity is discussed later.

As for the circular spots on the surface of the 900°C-annealed Cu/TaN_x system, they can be divided into three regions according to their distinct appearances, and labeled as region I, region II, and region III (see Fig. 4a). Figure 5 shows magnified micrographs of the 900°C-annealed Cu/TaN_x/Ta/SiO_2/⟨Si⟩ sample at region I, II, and III, respectively. EDS analysis was used to identify the chemical compositions of these regions. To reduce the inaccuracy of the compositions influenced by the underlayer, the operating voltage of the electron beam was lowered to 10 kV so that the X-ray generation depth is less than 0.1 μm.

DOCKET ALARM Find authenticated court documents without watermarks at docketalarm.com.

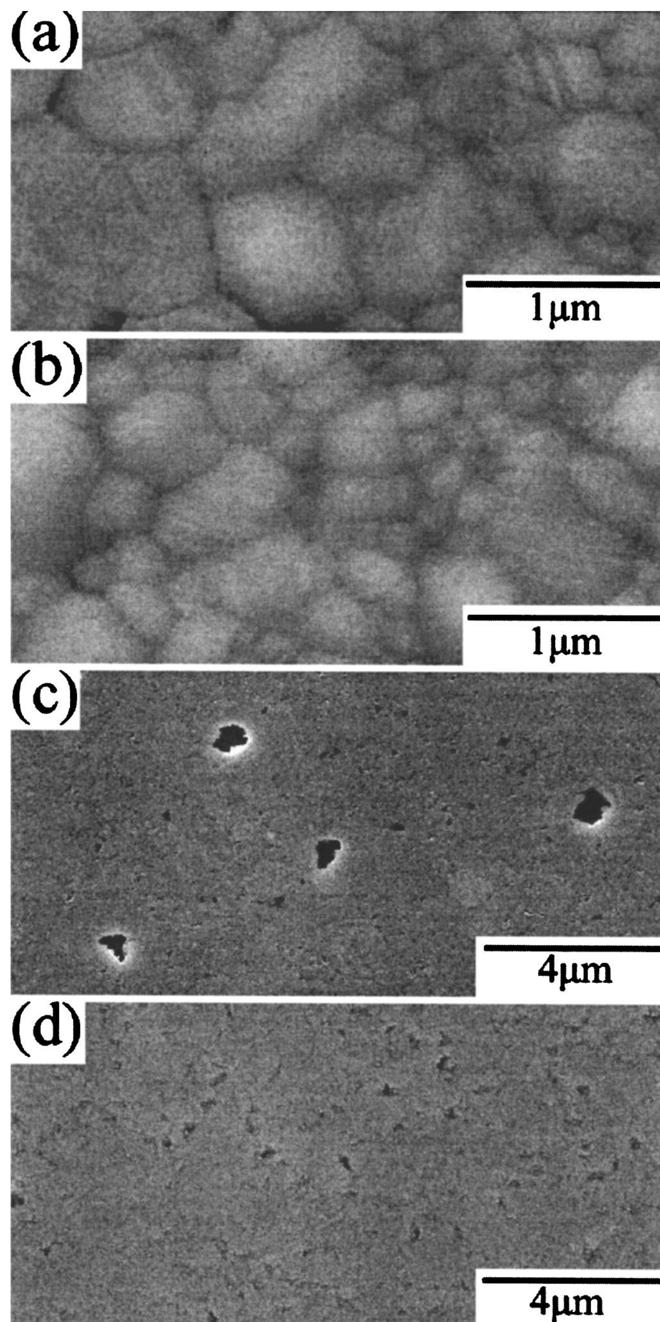

Figure 3. SEM images of the surfaces of (a) $Cu/TaN_x/Ta/SiO_2/\langle Si\rangle$, and (b) $Cu/TaN/Ta/SiO_2/\langle Si\rangle$ after annealing at 700°C and (c) $Cu/TaN_x/Ta/SiO_2/\langle Si\rangle$, and (d) $Cu/TaN/Ta/SiO_2/\langle Si\rangle$ after annealing at 800°C.

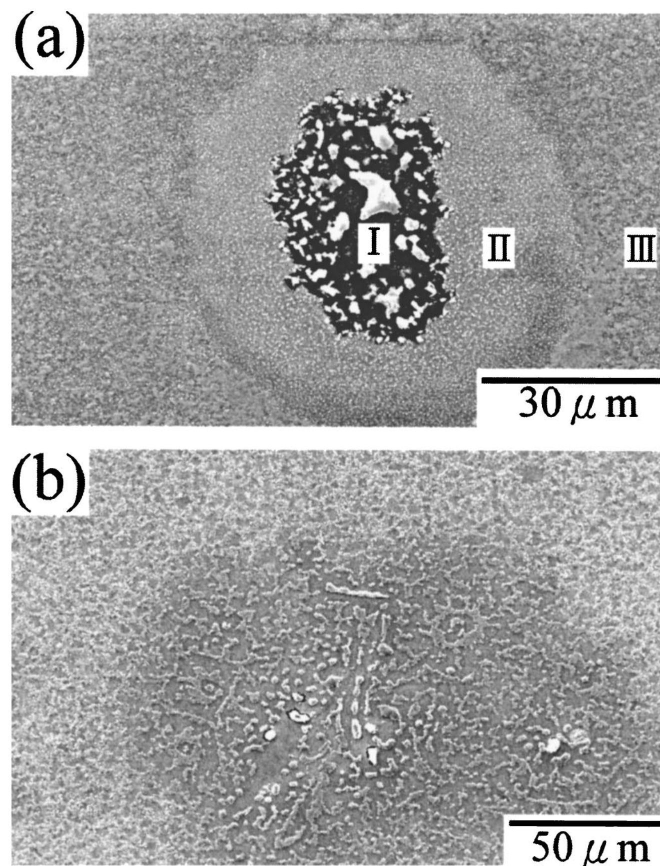

Figure 4. SEM images of the surfaces of (a) $Cu/TaN_x/Ta/SiO_2/\langle Si\rangle$ and (b) $Cu/TaN/Ta/SiO_2/\langle Si\rangle$ after annealing at 900°C.

The EDS spectrum shows that in region I (Fig. 5a), the large grains (labeled a) mainly consist of Cu. The major elements in the region labeled b are copper, silicon, and oxygen, indicating that the matrix in region I is the SiO_2 layer. This means that the top Cu layer and the underlaying TaN_x film had seriously deteriorated, therefore the SiO_2 layer was revealed in region I. The EDS spectrum in region II (area labeled c) consists of tantalum and oxygen (Fig. 5b). The low content of copper suggests that the grainy matrix observed in region II is the TaN_x film, and it may be oxidized. The TaN_x underlayer was revealed because the Cu top layer delaminated seriously after annealing at high temperature. At region III (Fig. 5c), the detected elements are Cu and Ta, for the area labeled as d and e, respectively. Therefore, the rough surface layer is Cu and the underlayer is TaN_x. In region III, copper layer agglomerated but still remained continuous in surface morphology. EDS analysis was also used to detect the composition distributions on the Cu/TaN sample surface (Fig. 4b) and the locations detected were labeled as a, b, and c in Fig. 6. Based on the EDS analysis, we have determined that the large grains and spherical clusters (locations labeled as a and c, respectively) on the surface of the Cu/TaN samples after annealing at high temperatures consist of Cu and O. Meanwhile, the matrix revealed on the surfaces of Cu/TaN samples (labeled as b) after annealing should be the TaN layer.

As regards interfacial diffusion, compositional depth profiles of the as-deposited and 700°C-annealed samples were investigated by RBS and the spectra are shown in Fig. 7. The RBS spectra of samples annealing at higher annealing temperatures (800 or 900°C) are not shown because the surface morphology of these samples is not uniform (scattered with voids or spots) so that they are not appropriate for RBS analysis. Figure 7 shows that there is a small Ta signal present on the surface of the $Cu/TaN_x/Ta/SiO_2/\langle Si\rangle$ sample after annealing at 700°C. The rest of the profile shifts slightly to the left due to the surface Ta. It had been reported that Ta has a very high affinity to oxygen and reacts with it to form Ta_2O_5.[21] Consequently, some Ta atoms may penetrate through the Cu layer to the surface to react with the residual oxygen in the annealing ambient. Except that, the Cu tail is a little slanting as compared to the as-deposited profile. It is said that as Ta diffused out to the surface, some vacancies would be left behind at the interface of Cu and TaN_x. Therefore, Cu atoms could diffuse into the TaN_x layer. Diffusion of Cu into the TaN_x layer is only minuscule, as shown in Fig. 7a. Furthermore, Ta diffusing through the extended defects, such as grain boundaries, would decorate and block the active paths for

DOCKET ALARM Find authenticated court documents without watermarks at docketalarm.com.

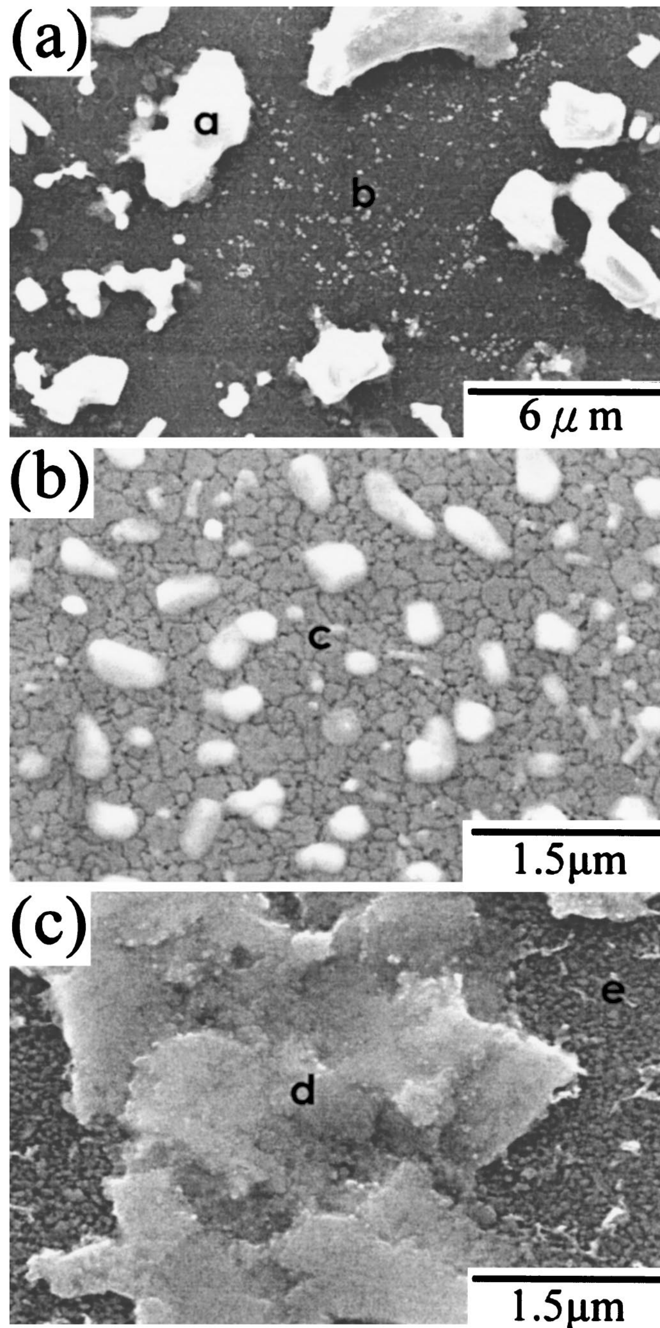

Figure 5. Magnified SEM images of the surfaces of (a) region I, (b) region II, and (c) region III in Cu/TaN_x/Ta/SiO_2/⟨Si⟩ after annealing at 900°C.

grain boundary diffusion. It will improve the capability to inhibit Cu from diffusing. On the other hand, no surface Ta signal is found in the RBS spectrum of the 700°C-annealed Cu/TaN/Ta/SiO_2/⟨Si⟩ sample, while the Ta profile becomes wide-spreading (Fig. 7b). Also, the copper tail becomes slanting, in a slightly higher degree than the previous system. The RBS profile indicates that interdiffusion occurred at the Cu/TaN and TaN/Ta/SiO_2 interfaces for the 700°C annealed Cu/TaN/Ta/SiO_2/⟨Si⟩ sample.

Crystallite sizes of TaN_x and TaN films were estimated by using the Scherrer equation[22] and presented in Table I. The crystallite sizes were calculated from the full-width at half maximum (fwhm) of the Ta_2N (101) peak and TaN (111) peak, respectively. The table indicates that the crystallite size of the TaN_x, which underwent the amorphous-to-crystalline transformation, increased drastically to

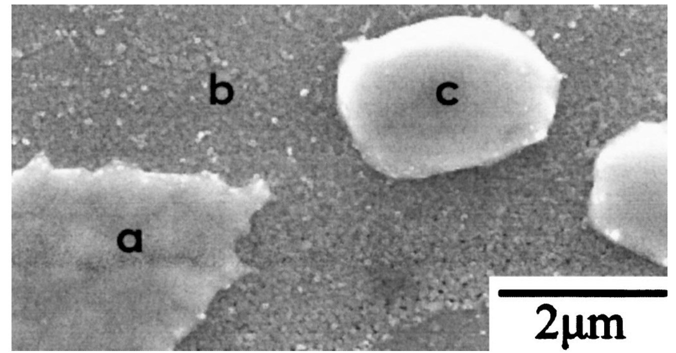

Figure 6. Magnified SEM images of the surface of Cu/TaN/Ta/SiO_2/⟨Si⟩ after annealing at 900°C.

20.5 nm after annealing at 900°C. However, the crystallite size of the 900°C-annealed polycrystalline TaN film was 14.2 nm, which was almost the same as that of the as-deposited TaN film (12.4 nm). In addition, Ta_2N has a melting point of 2050°C, compared with that of 3087°C for TaN. According to the empirical relationship, the activation energy of grain growth of Ta_2N is projected to be significantly lower than its TaN counterpart. Therefore, grain growth of Ta_2N is expected to be in evidence. According to Chaudhari's report,

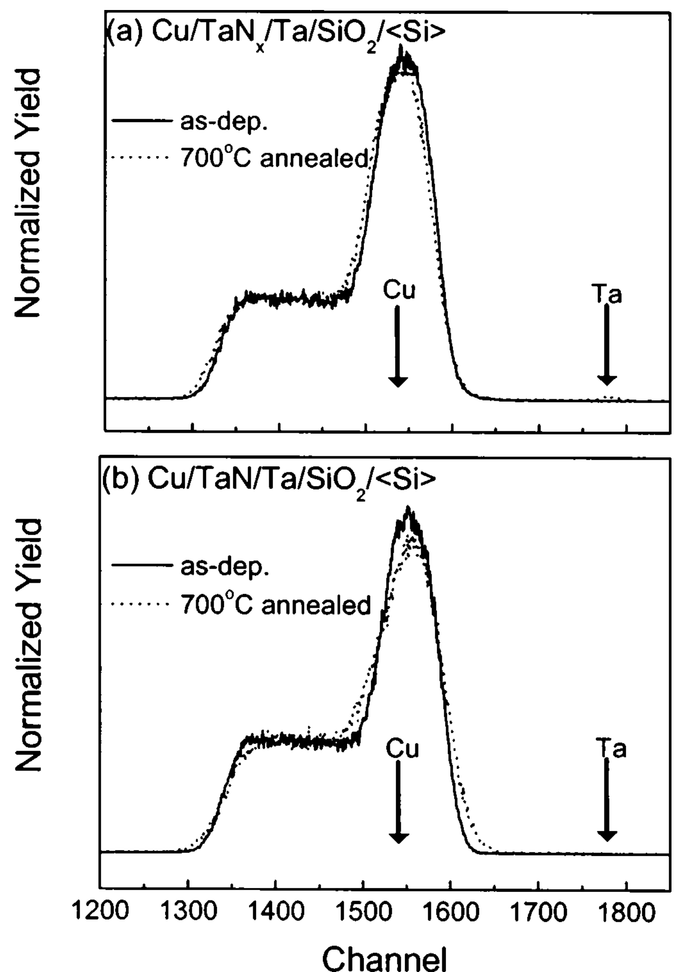

Figure 7. RBS spectra of the (a) Cu/TaN_x/Ta/SiO_2/⟨Si⟩ and (b) Cu/TaN/Ta/SiO_2/⟨Si⟩ samples, as deposited and after annealing at 700°C. The arrows indicate the backscattered energies of Cu and Ta on sample surface.

DOCKET ALARM
Find authenticated court documents without watermarks at docketalarm.com.

Table I. Estimated crystallite sizes of Ta-N films.

	Ta_2N (nm)	TaN (nm)
As-deposited	···	12.4
After annealing at 900°C	20.5	14.2

tensile stress will be produced in film as grains grow.[23] Furthermore, Chuang *et al.*[24] had reported that voids would be formed on the surfaces of Ta or Ta-N film to relieve the surface tension. In our study, the crystallite size of TaN_x apparently increased after annealing. Consequently, the as-deposited amorphous TaN_x film, which crystallized into a Ta_2N phase and underwent huge grain growth, must be stressed severely. To relieve the additional tensile stress, cracks or voids were formed. On the other hand, TaN film maintained similar crystallite size to the as-deposited film even after annealing at high temperature. This indicates that the TaN film sustained less tensile stress than the Ta_2N film did after annealing. Therefore, there were no apparent cracks and voids observed on the TaN film.

Now, we can infer a mechanism for the broken holes formed in the Cu/TaN_x system. At first, there may be some local defects existing in the thermally grown SiO_2 film, which could act as fast diffusion paths for copper to penetrate and then react with the Si substrate. However, the amorphous TaN_x diffusion barrier between copper and SiO_2 could prevent Cu from diffusing through it efficiently. After annealing at high temperatures, amorphous TaN_x film tended to crystallize into Ta_2N phases and was stressed severely so that lots of grain boundaries and voids formed. Consequently, the copper upper layer penetrated through the grain boundaries and voids in the TaN_x, and the defects in the SiO_2 film to the Si substrate and reacted with it. The broken holes were also observed by Holloway *et al.*[9] using Ta and Tsai *et al.*[17] using TaN. The difference between our experiments and their studies is that there is a SiO_2 layer between the diffusion barrier and the silicon substrate in this study. According to Tsai *et al.*, the gray dots might be the initial sites on the TaN film for copper to penetrate. In the present study, it indicated that the conditions for copper diffusing were not only the grain boundaries or defects in the barrier but also the SiO_2 underlayer.

The morphology of Cu in region II (Fig. 5b) was circular dots scattered on the TaN_x matrix. According to Miller *et al.*,[25] one of the important factors in determining the possibility of agglomeration is the ratio of the film thickness to the grain size. When the grain-size-to-film-thickness ratio exceeds a critical value, the breakup will lower the free energy of the system. Hence, copper tended to agglomerate seriously around the reaction spots because the process of copper penetrating through the defects in the center of the reaction spots leads to the copper layer becoming thinner and thinner. Therefore, the grain-size-to-film-thickness ratio in region II should be larger than it was in region III. This means that the copper layer in region II underwent a more serious agglomeration than region III and became round-shaped clusters as shown in Fig. 5b.

On the contrary, the Cu/TaN system still keeps the microstructure intact owing to minor grain growth even after annealing at 900°C. Therefore, no broken holes were observed on the surface of Cu/TaN/Ta/SiO_2/⟨Si⟩ samples.

Conclusion

The criteria to choose an appropriate diffusion barrier include not only low resistivity but also excellent integrity and capability for preventing copper from penetrating through it. Cu/TaN_x (amorphous, $x \approx 0.5$)/Ta/SiO_2/⟨Si⟩ samples possessed lower sheet resistances than Cu/TaN(crystalline)/Ta/SiO_2/⟨Si⟩ samples until annealing at 800°C. After annealing at 900°C, the sheet resistance value of Cu/TaN_x/Ta/SiO_2/⟨Si⟩ sample increased drastically, which was about twice as large as that of Cu/TaN/Ta/SiO_2/⟨Si⟩. By using SEM and EDS analyses, we found that the TaN_x film between Cu and SiO_2 bears an additional tensile stress because of its substantial grain growth, which makes voids produced in the TaN_x film after annealing at 900°C. These defects existing in the TaN_x film then resulted in apparent reaction spots on the surface of Cu. On the other hand, TaN grains did not grow apparently so that the TaN barrier can keep its integrity even after annealing at 900°C. However, at lower annealing temperatures, RBS spectra indicate that the TaN_x film has a better ability to prevent the copper diffusion due to the amorphous character of TaN_x. Therefore, we may conclude that the TaN_x film is more appropriate than the TaN film for applications in integrated circuits. Nevertheless, the TaN_x film degrades seriously after annealing at 900°C, indicating that TaN_x may be less sustainable than TaN when encountering a severe upsurge in temperature.

Acknowledgments

The authors gratefully acknowledge the financial support from the National Science Council of Taiwan (grant no. NSC-91-2216-E-006-059).

National Cheng Kung University assisted in meeting the publication costs of this article.

References

1. C. W. Park and R. W. Vook, *Appl. Phys. Lett.*, **59**, 175 (1991).
2. P. J. Pan and C. H. Ting, *IEEE Trans. Ind. Electron.*, **IE-29**, 154 (1982).
3. S. P. Murarka, *Mater. Sci. Eng., R.*, **19**, 87 (1997).
4. C. S. Liu and L. J. Chen, *J. Appl. Phys.*, **74**, 5501 (1993).
5. A. Cros, M. O. Aboelfotoh, and K. N. Tu, *J. Appl. Phys.*, **67**, 3328 (1990).
6. S. Q. Wang, I. J. M. M. Raaijmakers, B. J. Burrow, S. Suthar, S. Redkar, and K. B. Kim, *J. Appl. Phys.*, **68**, 5176 (1990).
7. K. C. Park, S. H. Kim, and K. B. Kim, *J. Electrochem. Soc.*, **147**, 2711 (2000).
8. E. Kolawa, J. S. Chen, J. S. Reid, P. J. Pokela, and M. A. Nicolet, *J. Appl. Phys.*, **70**, 1369 (1991).
9. K. Holloway, P. M. Fryer, C. Cabral, Jr., J. M. E. Harper, P. J. Bailey, and K. H. Kelleher, *J. Appl. Phys.*, **71**, 5433 (1992).
10. K. H. Min, K. C. Chun, and K. B. Kim, *J. Vac. Sci. Technol. B*, **14**, 3263 (1996).
11. G. S. Chen and S. T. Chen, *J. Appl. Phys.*, **87**, 8473 (2000).
12. K. M. Latt, Y. K. Lee, S. Li, T. Osopowicz, and H. L. Seng, *Mater. Sci. Eng., B*, **84**, 217 (2001).
13. K. M. Chang, T. H. Yeh, I. C. Deng, and C. W. Shin, *J. Appl. Phys.*, **82**, 1469 (1997).
14. J. E. Kelsey, C. Goldberg, G. Nuesca, G. Peterson, A. E. Kaloyeros, and B. Arkles, *J. Vac. Sci. Technol. B*, **17**, 1101 (1999).
15. A. E. Kaloyeros and E. Eisenbraun, *Annu. Rev. Mater. Sci.*, **30**, 363 (2000).
16. B. M. Ekstrom, S. Lee, N. Magtoto, and J. A. Kelber, *Appl. Surf. Sci.*, **171**, 275 (2001).
17. M. H. Tsai, S. C. Sun, C. E. Tsai, S. H. Chuang, and H. T. Chiu, *J. Appl. Phys.*, **79**, 6932 (1996).
18. Y. K. Lee, K. M. Latt, J. H. Kim, T. Osipowicz, S. Y. Chaim, and K. S. Lee, *Mater. Sci. Eng., B*, **77**, 282 (2000).
19. H. Wang, A. Tiwari, X. Zhang, A. Kvit, and J. Narayan, *Appl. Phys. Lett.*, **81**, 1453 (2002).
20. C. C. Chang, J. S. Jeng, and J. S. Chen, *Thin Solid Films*, **413**, 46 (2002).
21. K. Holloway and P. M. Fryer, *Appl. Phys. Lett.*, **57**, 1736 (1990).
22. B. D. Cullity and S. R. Stock, *Elements of X-Ray Diffraction*, 3rd ed., p. 170, Prentice Hall, New Jersey (2001).
23. P. Chaudhari, *J. Vac. Sci. Technol.*, **9**, 520 (1971).
24. J. C. Chuang and M. C. Chen, *Thin Solid Films*, **322**, 213 (1998).
25. K. T. Miller, F. F. Lange, and D. B. Marshall, *J. Mater. Res.*, **5**, 151 (1990).

DOCKET ALARM Find authenticated court documents without watermarks at docketalarm.com.